A Study of Lateral Vehicle Control Under a 'Virtual' Force Framework

Eric J. Rossetter

Design Division
Department of Mechanical Engineering
Stanford University
Stanford, California 94305-4021
Email: ejross@cdr.stanford.edu

J. Christian Gerdes

Design Division
Department of Mechanical Engineering
Stanford University
Stanford, California 94305-4021
Email: gerdes@cdr.stanford.edu

Abstract

Future automotive safety functions, such as lanekeeping and collision avoidance, link the vehicle dynamically to its environment. As a result, a combination of the mechanical system dynamics and the virtual link to the roadway or obstacles determines the vehicle motion. This paper looks at the combined influence of decoupling lateral and yaw modes, preview distance, and controller damping on the stability and performance of lateral controllers. The effects of these characteristics are studied using an intuitive 'virtual' forces analogy where the control inputs are viewed as a single force acting on the vehicle. With the ability to influence the coupling between lateral and yaw modes, the 'virtual' control force can be shifted along the length of the vehicle. For stability, this force must be applied in front of the neutral steer point. In addition, shifting this control force can give satisfactory system behavior with a minimal preview distance. The benefits of lookahead are also explored under this framework, giving well behaved responses without the addition of controller damping. The combination of lookahead and damping on the velocity states allows complete freedom in designing the system response.

1 Introduction

As automobiles incorporate new drive-by-wire technologies it will be possible to implement lateral controllers on passenger vehicles for collision avoidance and lanekeeping [1] [2]. Research in lateral control has focused on four main factors that influence system performance: vehicle handling characteristics, preview distance, actuator capability, and controller design. Understanding the interaction of all these factors is crucial in the design of lateral control systems.

Vehicle handling characteristics is a key component in control system design. Open-loop vehicle stability is well understood and research in this area dates back to the early 1930's. At this time, researchers at General Motors first noticed that some steering geometries created a tendency for the vehicle to 'oversteer' the desired trajectory. Shortly after this discovery, the same 'oversteering' behavior was noticed with vehicles that had underinflated rear tires or a rearward weight bias. This nurtured the study of tire dynamics and their influence on vehicle handling. Stonex [3] was one of the first to study steady-state vehicle stability and explore understeering and oversteering behavior. This led to the development and analysis of dynamic vehicle models, resulting in a mathematical understanding of understeering and oversteering behavior [4]. The results showed that understeering vehicles are always stable but damping decreases with increasing speed. Oversteering vehicles, however, are stable with increasing damping up to a critical speed where the vehicle becomes

unstable [5] [6]. The simple models that yield these results are still used for most vehicle control systems design.

With sensor and computer advances, the capability for vehicle control became possible. Fenton [7] did initial work in vehicle lateral control by using an electric wire as a reference. In this work, the vehicle only had knowledge of its current lateral position, which created instability at high speeds. These look-down reference systems were also studied by researchers at PATH [8] and later by Guldner et al. [9] but still had instabilities above 30 m/s. In order to achieve speeds appropriate for highway travel, it is necessary to incorporate a look-ahead reference. The advantage of incorporating a preview distance was shown theoretically by Peng and Tomizuka [10] and experimentally by Alleyne and DePoorter [11]. Guldner et al. [12] created a 'virtual' preview distance for high speed stability using a look-down reference at the front and rear of the vehicle.

With additional actuators such as four wheel steering or differential braking, it is possible to change the coupling between lateral and yaw modes. Ackermann [13] developed control algorithms that decouple the lateral and yaw dynamics to make the driving experience safer and more comfortable. Alleyne [14] looked at lateral control of a vehicle using various combinations of steering and differential braking for improved lanekeeping. The ability to alter the coupling between the yaw and lateral modes adds another degree of freedom in the control system design. In order to study the interaction of all these different variables it is convenient to look at control from a 'virtual' force standpoint. In essence, most control laws can be viewed as the combination of external forces and torques applied at the center of gravity. This can be combined into a single virtual control force acting at some point along the longitudinal axis of the vehicle. This virtual force concept gives physical insight into controller design that is extremely useful for many types of control applications.

This paper presents a stability analysis illustrating the influence of the following attributes on the stability and performance of lateral vehicle control.

- Vehicle Handling Properties (Amount of Understeer/Oversteer)
- Virtual Force Application Point (Coordination of Steering and Braking)
- Sensing Location (Amount of Lookahead)
- Controller Damping

The results clearly illustrate that the virtual control force must be applied in front of the neutral steer point for stability. Adequate system response can then be achieved by incorporating an appropriate amount of lookahead. The combination of lookahead and controller damping allows complete control over the system response. These results provide insight into the proper way of applying virtual forces to control high speed vehicles.

2 Vehicle Dynamics

The vehicle model used in the analysis is a simple three degree of freedom yaw plane representation with differential braking, shown in Figure 1.

$$
\begin{aligned}
m\dot{U}_x &= F_{xr} + F_{xf}cos\delta - F_{yf}sin\delta + mrU_y && (1)\\
m\dot{U}_y &= F_{yr} + F_{xf}sin\delta + F_{yf}cos\delta - mrU_x && (2)\\
I_z\dot{r} &= aF_{xf}\sin\delta + aF_{yf}\cos\delta - bF_{yr} && (3)\\
&+ \frac{d}{2}(\Delta F_{xr} + \Delta F_{xf}\cos\delta)
\end{aligned}
$$

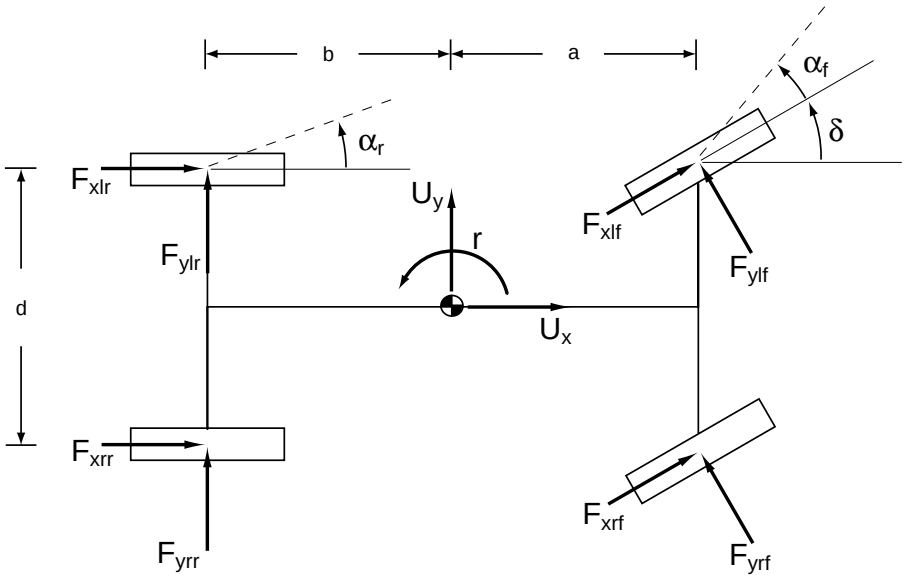

Figure 1: Vehicle Model

where

$$F_{xf} = F_{xrf} + F_{xlf} \tag{4}$$
$$F_{xr} = F_{xrr} + F_{xlr} \tag{5}$$
$$\Delta F_{xf} = F_{xrf} - F_{xlf} \tag{6}$$
$$\Delta F_{xr} = F_{xrr} - F_{xlr} \tag{7}$$

Assuming small angles and equal slip angles on the left and right wheels,

$$\alpha_f = \frac{U_y + ra}{U_x} - \delta \tag{8}$$
$$\alpha_r = \frac{U_y - rb}{U_x} \tag{9}$$

Using a linear tire model, the lateral forces are given as

$$F_{yf} = -C_f \alpha_f \tag{10}$$
$$F_{yr} = -C_r \alpha_r \tag{11}$$

where C_f and C_r are the front and rear cornering stiffnesses, respectively. Substituting the expressions for the lateral forces into Equations 1 through 3 and making small angle approximations yields,

$$m\dot{U}_x = mrU_y + F_{xr} + F_{xf} + C_f(\frac{U_y + ra}{U_x})\delta \tag{12}$$
$$m\dot{U}_y = -C_r(\frac{U_y - rb}{U_x}) - C_f(\frac{U_y + ra}{U_x}) - mrU_x + C_f\delta + F_{xf}\delta \tag{13}$$
$$I_z\dot{r} = aF_{xf}\delta - aC_f(\frac{U_y + ra}{U_x}) + bC_r(\frac{U_y - rb}{U_x}) + aC_f\delta + \frac{d}{2}(\Delta F_{xr} + \Delta F_{xf}) \tag{14}$$

Assuming a vehicle that has throttle, brake, and steer-by-wire capabilities so that steering, braking and two drive wheels can be controlled, the equations can be rewritten as

$$M\ddot{q} = f(\dot{q}) + g(\dot{q}, u_c) \tag{15}$$

where $\dot{q} = [U_x\ U_y\ r]^T$ and the control vector $u_c = [\delta\ F_{xrf}\ F_{xlf}\ F_{xrr}\ F_{xlr}]^T$. M is the positive definite mass matrix, $f(\dot{q})$ contains the terms that are not influenced by the control vector and $g(\dot{q}, u_c)$ has the remaining controlled terms.

$$\begin{aligned} M &= \begin{bmatrix} m & 0 & 0 \\ 0 & m & 0 \\ 0 & 0 & I_z \end{bmatrix} \\ f(\dot{q}) &= \begin{bmatrix} mrU_y \\ -C_r(\frac{U_y - rb}{U_x}) - C_f(\frac{U_y + ra}{U_x}) - mrU_x \\ -aC_f(\frac{U_y + ra}{U_x}) + bC_r(\frac{U_y - rb}{U_x}) \end{bmatrix} \\ g(\dot{q}, u_c) &= \begin{bmatrix} F_{xr} + F_{xf} + C_f(\frac{U_y + ra}{U_x})\delta \\ C_f\delta + F_{xf}\delta \\ aF_{xf}\delta + aC_f\delta + \frac{d}{2}(\Delta F_{xr} + \Delta F_{xf}) \end{bmatrix} \end{aligned}$$

The controlled terms, $g(\dot{q}, u_c)$, are then set equal to the desired control forces. This set of equations can then be used to solve for the control vector, u_c [16].

3 Virtual Force Analogy for Control

In this paper, the virtual control force is realized through a combination of differential braking and front steering. Figure 2 shows how forces derived from the control inputs (differential braking and front steering) can be thought of as a virtual control force. This is accomplished by creating an equivalent force system consisting of a longitudinal and lateral force on the vehicle. For lateral control, the longitudinal force is small and disappears in the linearization of the system dynamics (Section 4). The ability to manipulate the coupling between lateral and yaw modes allows movement of the virtual control force along the longitudinal axis of the vehicle. For example, if differential braking is unavailable ($\Delta F_{xf} = \Delta F_{xf} = 0$), the virtual control force from the steering angle is constrained at the front axle. With differential braking, the moment equation can be influenced independently from steering, effectively shifting the location of the virtual force from the front axle.

For general vehicle control, the virtual force is described in global coordinates $w = [s\ e\ \psi]^T$ where s is the distance along the roadway, e is the distance of the vehicle's center of gravity from the lane center and ψ is the heading angle (Figure 3). Transformation between the global and body fixed coordinates is achieved with

$$\frac{\partial \dot{w}}{\partial \dot{q}} = \frac{\partial w}{\partial q} = \begin{bmatrix} \cos\psi & -\sin\psi & 0 \\ \sin\psi & \cos\psi & 0 \\ 0 & 0 & 1 \end{bmatrix} \tag{16}$$

In this paper, the virtual force is based on a simple proportional derivative control law. For general vehicle control

$$F_{virtual} = -K\omega - D\dot{\omega} \tag{17}$$

where K is the proportional gain matrix and D is the damping matrix. These control forces are oriented in global coordinates and must be transformed to vehicle fixed coordinates to solve for the

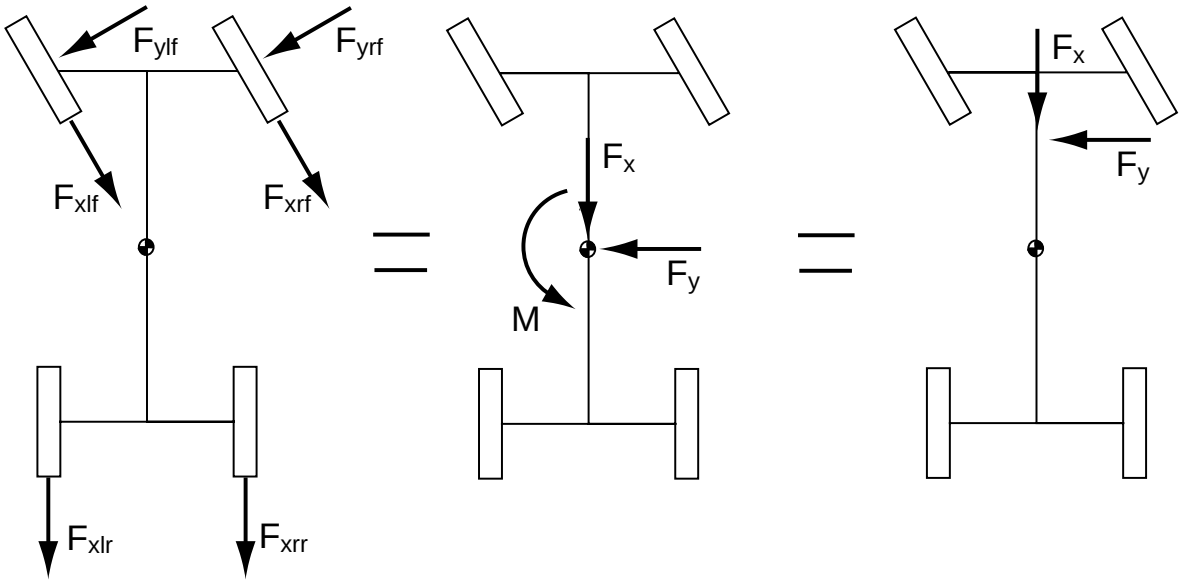

Figure 2: Virtual Force Analogy

actual control inputs (steering angle and differential braking).

$$g(\dot{q}, u_c) = \left[(-K\omega - D\dot{\omega})^T \frac{\partial \omega}{\partial q}\right]^T \tag{18}$$

With this controller, the vehicle dynamics can be rewritten, replacing the control input vector with the virtual control force:

$$M\ddot{q} = f(\dot{q}) + \left[(-K\omega - D\dot{\omega})^T \frac{\partial \omega}{\partial q}\right]^T \tag{19}$$

The system dynamics now consist of virtual forces and the drift term containing the vehicle dynamics not directly influenced by control inputs. This control law is analogous to having virtual forces from lateral, longitudinal, and torsional springs and dampers. This spring and damper analogy is similar to work done by Hennessey et al. [17] and Schiller et al. [18][19] in the design of a 'virtual bumper'. If an obstacle penetrates the bumper, imaginary springs and dampers are compressed applying a virtual force to the vehicle. In this paper, however, only the lateral direction is used for lanekeeping (Figure 4).

This set of non-linear differential equations is the focus of the analysis. The behavior in question is the stability of the vehicle with respect to a desired trajectory consisting of a constant longitudinal velocity in the center of the road. Since the interesting behavior is in global coordinates, it makes sense to transform the equations of motion into global states and then linearize the system about the desired trajectory.

4 Virtual Force at C.G.

The goal of the stability analysis is to study the vehicle's response to small incursions from the lane center. The basic idea is to transform the equations of motion into the global reference frame and then rewrite the three second order differential equations as six first order equations that are functions of the global coordinates and their derivatives. Jacobian linearization can then be performed about a straight trajectory where the longitudinal velocity is a constant S and all other states are zero.

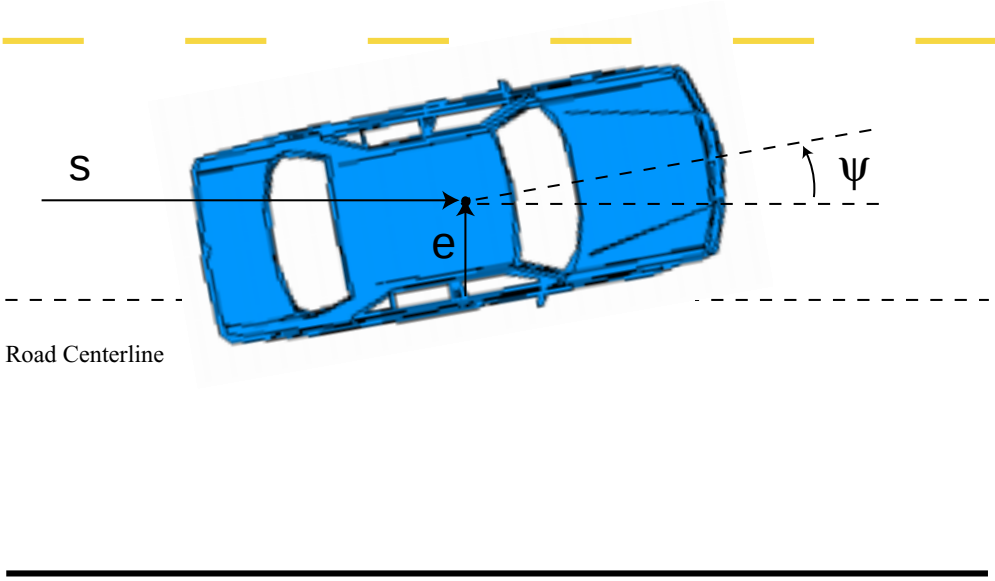

Figure 3: Global Coordinates

Without a virtual force, this analysis returns well-known stability results for vehicle handling, as should be expected. The interaction between vehicle handling, virtual force application point, and sensor location is shown without adding any artifical damping ($D = 0$). This control force is only dependent on the lateral position of the vehicle from the lane center.

$$F_{virtual} = -ke \tag{20}$$

The basic analysis raises stability concerns about the controlled system that can be resolved by shifting the application of the virtual force and sensing location. In the final section, artificial damping is added, creating a virtual force based on a proportional derivative (PD) control law.

4.1 Linearization Without a Virtual Force

The linearization of a vehicle about a constant longitudinal velocity gives,

$$\delta\dot{x} = A\delta x \tag{21}$$

where $\delta x = [\delta e\ \delta\dot{e}\ \delta\psi\ \delta\dot{\psi}]^T$ are perturbations away from the nominal states and

$$A = \begin{bmatrix} 0 & 1 & 0 & 0 \\ 0 & \frac{-(C_f+C_r)}{mS} & \frac{C_f+C_r}{m} & \frac{(-aC_f+bC_r)}{mS} \\ 0 & 0 & 0 & 1 \\ 0 & \frac{(-aC_f+bC_r)}{I_zS} & \frac{(aC_f-bC_r)}{I_z} & \frac{-(a^2C_f+b^2C_r)}{I_zS} \end{bmatrix} \tag{22}$$

Taking the determinant of $(\lambda I - A)$ yields the characteristic equation of the system.

$$\lambda^2\left(\lambda^2 + \lambda a_1 + a_2\right) = 0 \tag{23}$$

where,

$$\begin{aligned} a_1 &= \frac{(C_f + C_r)I_z + (a^2C_f + b^2C_r)m}{I_zmS} \\ a_2 &= \frac{C_fC_r(a+b)^2 + (bC_r - aC_f)mS^2}{I_zmS^2} \end{aligned}$$

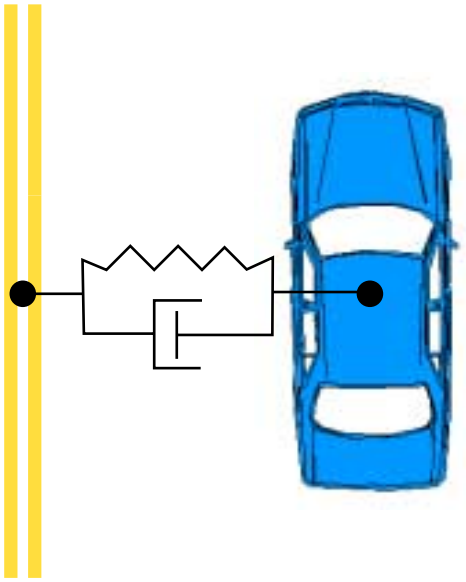

Figure 4: Lanekeeping Analogy

From the above equation, there are four eigenvalues. Two of these eigenvalues determine the vehicle handling and the two zero eigenvalues arise from the integrators for the positional states. In an understeering car (where $C_r b > aC_f$) both coefficients a_1 and a_2 are positive which, for a second order system, is sufficient to prove stability. In an oversteering case ($aC_f > bC_r$), the coefficient a_2 will be negative when the speed

$$S > \sqrt{\frac{C_f C_r (a+b)^2}{(aC_f - bC_r)m}} \tag{24}$$

This is the well known critical speed for an oversteering vehicle (Gillespie (1992)). As expected, the transformation to global coordinates did not change the basic stability properties of the vehicle: the understeering vehicle is always stable and the oversteering vehicle is stable below a critical speed.

4.2 Linearization With a Virtual Force

Adding a virtual control force in the form of Equation 19 yields a linear system which has the control force appearing in the lateral equation of motion. This adds one extra term to the matrix in Equation 22.

$$A = \begin{bmatrix} 0 & 1 & 0 & 0 \\ -\frac{\mathbf{k}}{\mathbf{m}} & -\frac{C_f+C_r}{mS} & \frac{C_f+C_r}{m} & \frac{(-aC_f+bC_r)}{mS} \\ 0 & 0 & 0 & 1 \\ 0 & \frac{(-aC_f+bC_r)}{I_z S} & \frac{(aC_f-bC_r)}{I_z} & \frac{-(a^2C_f+b^2C_r)}{I_z S} \end{bmatrix} \tag{25}$$

The characteristic equation is now

$$\lambda^4 + \lambda^3 b_1 + \lambda^2 b_2 + \lambda b_3 + b_4 = 0 \tag{26}$$

where

$$\begin{aligned} b_1 &= \frac{(C_f + C_r)I_z + (a^2 C_f + b^2 C_r)m}{I_z m S} \\ b_2 &= \frac{C_f C_r (a+b)^2 + (bC_r - aC_f)mS^2 + kI_z S^2}{I_z m S^2} \end{aligned}$$

	Understeer	Oversteer
m (kg)	1640	1640
I_z (N/m^2)	3500	3500
C_f (N/rad)	100000	100000
C_r (N/rad)	160000	80000
K	5000	5000
a (m)	1.3	1.3
b (m)	1.5	1.5

Table 1: Vehicle Parameters

$$\begin{aligned} b_3 &= \frac{k(a^2C_f + b^2C_r)}{I_z m S} \\ b_4 &= \frac{k(bC_r - aC_f)}{I_z m} \end{aligned}$$

Regardless of the vehicle's speed, the last term, b_4, is always negative when oversteering parameters are used. Sign changes in the characteristic equation coefficients fail the necessary conditions for stability. The addition of the virtual force alters the oversteering vehicle dynamics to produce instability by lowering the critical speed to zero. This instability occurs because the virtual force is applied at the center of gravity, causing the vehicle to turn into the applied force. This type of response is well known for an oversteering car with a physical force, such as a side wind, applied at the c.g.

If the vehicle is understeering, all the coefficients are positive. Although this is a necessary condition for stability, it is not sufficient. Using the Routh array, it can be shown that the system is stable up to a critical velocity.

$$S_{cr} = \left(\frac{N}{D}\right)^{1/2} \tag{27}$$

where N and D are

$$\begin{aligned} N &= -(a+b)^2 C_f C_r (a^2C_f + b^2C_r)(I_z(C_f + C_r) + (a^2C_f + b^2C_r)m) \\ D &= (C_f + C_r)I_z((C_f + C_r)(aC_f - bC_r)I_z + 2I_z K(a^2C_f + b^2C_r) \\ &+ (aC_f - bC_r)(a^2C_f + b^2C_r)m) \end{aligned}$$

Using the understeering parameters in Table 1 the critical speed is $27.06 m/s$. Figure 5 shows the understeering and oversteering response with the proportional controller. The initial conditions for the simulation are $e = 0.5m$ and $S = 25m/s$, representing a typical driving speed and an initial offset from the lane center. All other states are zero and the parameters used are in Table 1.

The results shown in Figure 5 show the exact behavior predicted by the linear analysis. The understeering vehicle is stable but underdamped, oscillating about the lane center. An oversteering vehicle exhibits drastically different results. The control force initially pushes the car towards the center of the lane, but the change in the vehicle dynamics causes a rotation into the applied force.

In the above analysis, the vehicle is controlled by a virtual force applied at the c.g. of the vehicle with sensing based on the lateral position of the c.g. The location of this control force results in instability for the oversteering vehicle that cannot be rectified by adding lookahead or controller damping. The only solution is to shift the control force forward until stability is achieved. For the understeering vehicle, this control strategy results in stability below a critical speed. The low damping characteristics and a critical speed within the operating range of the vehicle can be

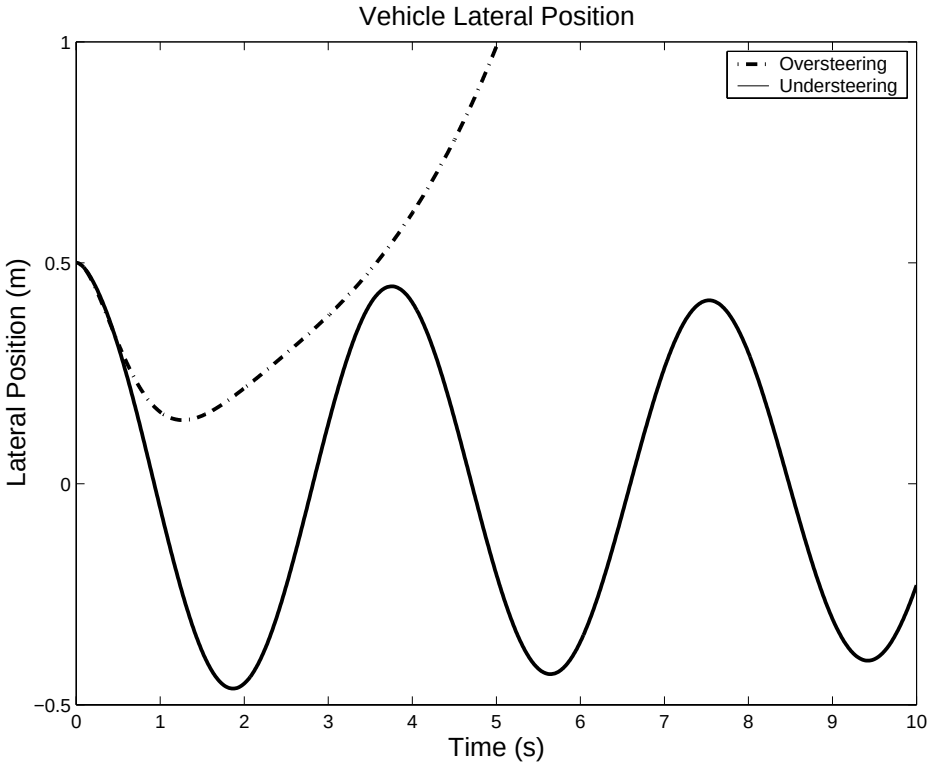

Figure 5: Simulation: Virtual Force at C.G.

attributed to sensing at the c.g. (i.e. no lookahead). An interesting result is that without any lookahead the critical speed is fairly large compared with previous results for look-down lateral controllers. This is a result of applying the control force at a location that almost decouples the lateral and yaw modes of the vehicle. This ability presents the option of producing adequate vehicle response without lookahead.

5 Shifting the Virtual Force

With the virtual control force acting at a distance, x_{cf}, in front of the c.g., the equations of motion have an extra term appearing in the moment equation.

$$A = \begin{bmatrix} 0 & 1 & 0 & 0 \\ -\frac{k}{m} & \frac{-(C_f+C_r)}{mS} & \frac{C_f+C_r}{m} & \frac{(-aC_f+bC_r)}{mS} \\ 0 & 0 & 0 & 1 \\ \frac{-\mathbf{kx_{cf}}}{\mathbf{I_z}} & \frac{(-aC_f+bC_r)}{I_zS} & \frac{(aC_f-bC_r)}{I_z} & \frac{-(a^2C_f+b^2C_r)}{I_zS} \end{bmatrix} \tag{28}$$

The characteristic equation is

$$\lambda^4 + \lambda^3 c_1 + \lambda^2 c_2 + \lambda c_3 + c_4 = 0 \tag{29}$$

where

$$\begin{aligned} c_1 &= \frac{(C_f + C_r)I_z + (a^2C_f + b^2C_r)m}{I_z m S} \\ c_2 &= \frac{C_f C_r (a+b)^2 + (bC_r - aC_f)mS^2 + kI_z S^2}{I_z m S^2} \end{aligned}$$

$$
\begin{aligned}
c_3 &= \frac{k(a^2C_f + b^2C_r + x_{cf}(bC_r - aC_f))}{I_z m S} \\
c_4 &= \frac{k(bC_r - aC_f + x_{cf}(C_f + C_r))}{I_z m}
\end{aligned}
$$

From the last section, the final term in the characteristic equation is sensitive to changes in the handling properties of the vehicle. With the ability to shift the virtual force it is possible to negate this problem. For stability, the following inequality must be satisfied.

$$bC_r - aC_f + (C_f + C_r)x_{cf} > 0 \tag{30}$$

so,

$$x_{cf} > \frac{aC_f - bC_r}{C_f + C_r} \tag{31}$$

The right hand side of the above expression is the definition of the neutral steer point, which has physical significance in vehicle dynamics. The neutral steer point is the location on the centerline of a vehicle where an external force will produce no steady state yaw velocity. This concept is often used to discuss sidewind sensitivity of a vehicle and has a natural interpretation when considering virtual forces and stability. For stability, the virtual force must be applied in front of the neutral steer point of the vehicle. This ensures that the vehicle will yaw in the same direction as the virtual control force.

If the virtual force is applied at the neutral steer point, the system is marginally stable with three negative eigenvalues and one at the origin. The coefficients for the characteristic equation become

$$
\begin{aligned}
c_1' &= \frac{(C_f + C_r)I_z + (a^2C_f + b^2C_r)m}{I_z m S} \\
c_2' &= \frac{C_f C_r (a+b)^2 + (bC_r - aC_f)mS^2 + kI_z S^2}{I_z m S^2} \\
c_3' &= \frac{kC_f C_r (a+b)^2}{(C_f + C_r)I_z m S} \\
c_4' &= 0
\end{aligned}
$$

With the virtual force at the neutral steer point there is still the possibility of a critical speed. The only term in this system which can possibly go negative for an oversteering vehicle is c_2'. From looking at the Routh array, the system actually has a critical speed that occurs before c_2' becomes negative.

$$S_{cr} = \left(\frac{N}{D}\right)^{1/2} \tag{32}$$

where

$$
\begin{aligned}
N &= -(a+b)^2 C_f C_r (C_f + C_r)(I_z(C_f + C_r) + (a^2C_f + b^2C_r)m) \\
D &= 2(C_f + C_r)^2 I_z^k - I_z(aC_f - bC_r)((C_f + C_r)^2 + k(bC_r - aC_f))m \\
&- (C_f + C_r)(aC_f - bC_r)(a^2C_f + b^2C_r)m^2
\end{aligned}
$$

Using the oversteering parameters in Table 1, their happens to be no critical speed for the system (the solution to Equation 32 is imaginary but certain oversteering parameters can give real critical speeds). By shifting the force to the neutral steer point, the oversteering vehicle is marginally stable, but exhibits a nicely damped response as compared with the understeering vehicle from the previous section (Figure 6). Since this control force location creates no steady state yaw velocity

there is minimal rotation, yielding an acceptable response. Shifting the control force to the neutral steer point of the understeering gives similar results (Figure 6)). The understeering vehicle has an overdamped response that is due to the transient behavior of the vehicle as it reaches steady state.

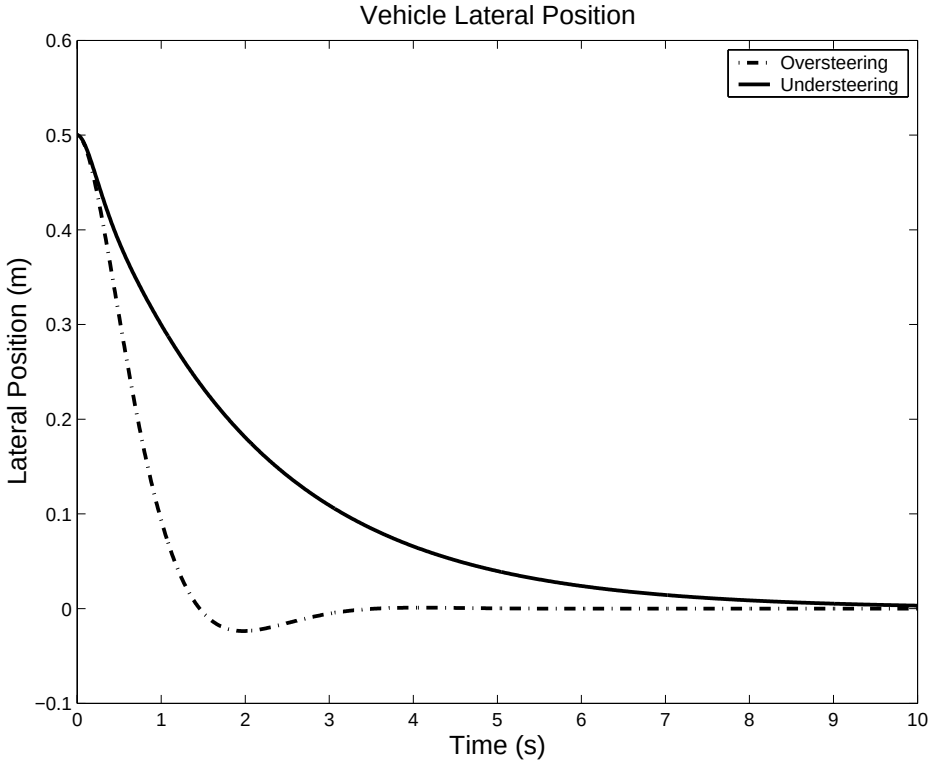

Figure 6: Simulation: Virtual Force at Neutral Steer Point

Figure 7 and Figure 8 show how the eigenvalues shift for an oversteering and understeering car as the virtual force is shifted from $0.5m$ behind the neutral steer point to $0.5m$ in front of the neutral steer point. The square denotes the initial position behind the neutral steer point. The eigenvalues verify that the system is unstable when the application point is behind the neutral steer point. As the virtual force is shifted forward, the system becomes stable, but as the force is moved further forward the system becomes oscillatory and eventually unstable. This instability is due to the lack of lookahead in the system.

Interestingly, in the case discussed in this section, the force is shifted to the neutral steer point but the sensing location remaines at the c.g. Therefore, in the oversteering case the sensing location is actually behind the control force while in the understeering vehicle it is slightly in front of this control force. In either case, with hardly any lookahead the system response is excellent. The limitation is that the neutral steer point is only marginally stable, yielding an eigenvalue at zero. If the control force is moved slightly rearward, the system will become unstable. It is unlikely that the vehicle parameters can be known with the accuracy necessary to pin point this location. Even variations in vehicle loading or tire pressure can shift this point and create instability. To be robust to parameter uncertainties the control force should be shifted in front of the neutral steer point.

As this force is moved towards the front axle of the vehicle, the damping lowers and a critical speed exists. The system response can be improved by incorporating an appropriate amount of lookahead. The role of lookahead in vehicles with the control force at the front axle (corresponding to having only steering) is well known but with the ability to shift the force there are two different

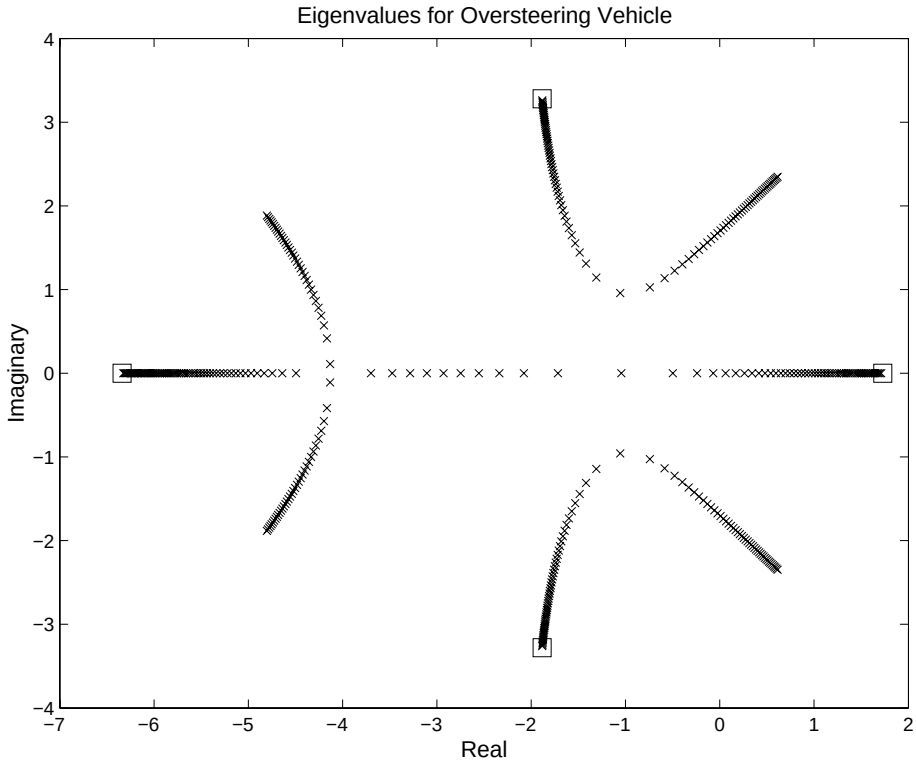

Figure 7: Oversteering Vehicle Eigenvalues as Application Point Shifts Forward

variables that influence stability and system behavior.

6 Incorporating Lookahead

In order to incorporate lookahead, the control force must depend on a lateral position that is in front of the application point. Defining e_{la} to be the projected lateral position a distance x_{la} in front of the c.g., as shown in Figure 9, yields the following control force.

$$F_{virtual} = -ke_{la} = -k(e + x_{la}sin(\psi)) \tag{33}$$

If small angle approximations are made, this expression for lookahead can be included in the linearized vehicle model.

$$A = \begin{bmatrix} 0 & 1 & 0 & 0 \\ -\frac{k}{m} & \frac{-(C_f+C_r)}{mS} & \frac{C_f+C_r}{m} - \mathbf{\frac{kx_{la}}{m}} & \frac{(-aC_f+bC_r)}{mS} \\ 0 & 0 & 0 & 1 \\ \frac{-kx_{cf}}{I_z} & \frac{(-aC_f+bC_r)}{I_zS} & \frac{(aC_f-bC_r)}{I_z} - \mathbf{\frac{kx_{la}x_{cf}}{I_z}} & \frac{-(a^2C_f+b^2C_r)}{I_zS} \end{bmatrix} \tag{34}$$

The characteristic equation is

$$\lambda^4 + \lambda^3 d_1 + \lambda^2 d_2 + \lambda d_3 + d_4 = 0 \tag{35}$$

where

$$d_1 = \frac{(C_f + C_r)I_z + (a^2C_f + b^2C_r)m}{I_z mS}$$

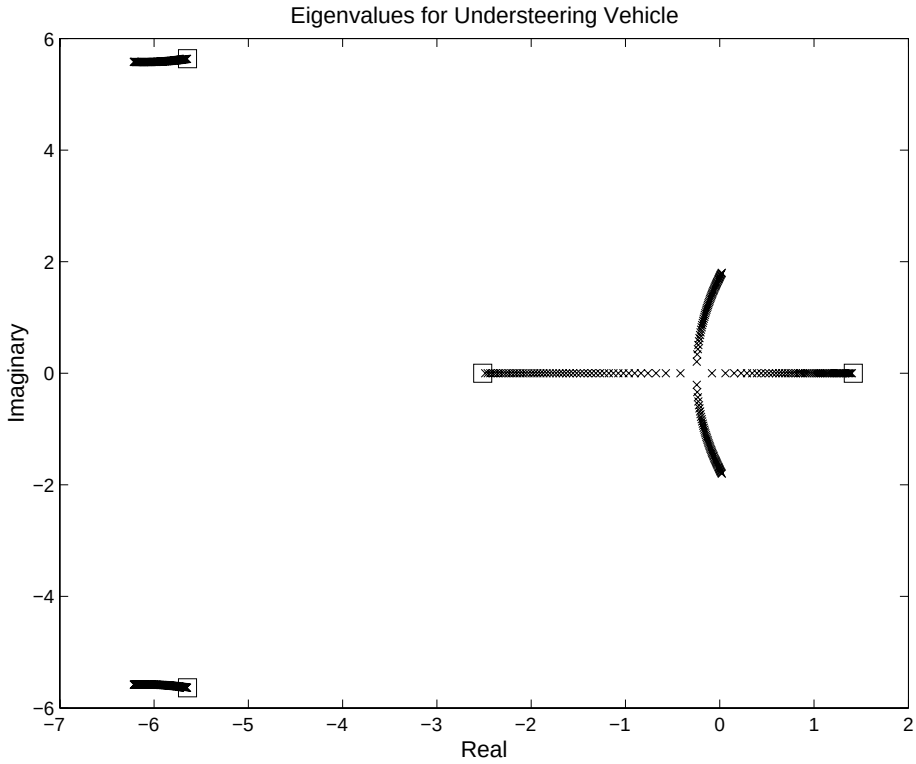

Figure 8: Understeering Vehicle Eigenvalues as Application Point Shifts Forward

$$
\begin{aligned}
d_2 &= \frac{C_f C_r (a+b)^2 + (bC_r - aC_f) m S^2 + k S^2 (I_z + m x_{cf} x_{la})}{I_z m S^2} \\
d_3 &= \frac{k(a^2 C_f + b^2 C_r + (x_{cf} + x_{la})(bC_r - aC_f) + (C_f + C_r) x_{cf} x_{la})}{I_z m S} \\
d_4 &= \frac{k(bC_r - aC_f + x_{cf}(C_f + C_r))}{I_z m}
\end{aligned}
$$

Now there are two factors effecting stability: application point of the virtual force and lookahead distance. From the previous section there are clear limitations on the application point of the control force. Notice that the addition of lookahead does not effect the final term in the characteristic equation. Therefore, the instability caused by applying the virtual force behind the neutral steer point cannot be rectified using lookahead. Once stability has been achieved by applying the force in front of the neutral steer point, system response and critical speed are changed by manipulation of the sensing location.

Figure 10 shows how the system eigenvalues change as the lookahead is varied from the c.g. to a preview distance of $60m$ for an understeering vehicle. The speed is held at a constant $30m/s$ and the application point is applied $0.5m$ in front of the neutral steer point. Initially, the vehicle is unstable with a pair of eigenvalues in the right half plane. As the lookahead distance is increased, these unstable poles eventually migrate into the left half plane, stabilizing the system. Increasing the lookahead by too great a margin has some negative side effects on system performance. Eventually, two eigenvalues move onto the real axis while the other two eigenvalues move towards the imaginary axis, decreasing the system damping.

Figure 11 depicts the system eigenvalues for an oversteering vehicle using the same range of lookahead distances. As in the understeering case, the system is initially unstable with a pair of eigenvalues in the right half plane. As the lookahead is increased, this eigenvalue pair moves into

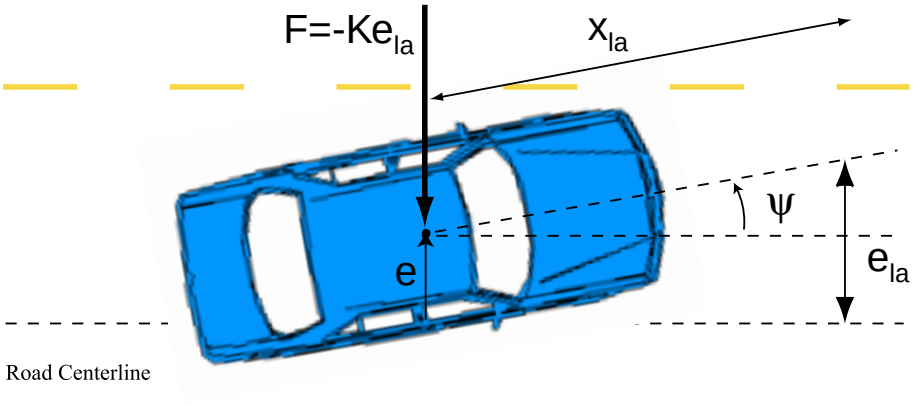

Figure 9: Lookahead

10 m Lookahead	**30 m Lookahead**	**50 m Lookahead**
-0.6748 + 2.0868i	-5.1086	-0.6163
-0.6748 - 2.0868i	-1.1999	-7.3928
-4.4865 + 5.1920i	-2.0071 + 5.7376i	-1.1568 + 6.9551i
-4.4865 - 5.1920i	-2.0071 - 5.7376i	-1.1568 - 6.9551i
ζ_{1-2}=0.3077	ζ_{1-2}=1.0	ζ_{1-2}=1.0
ζ_{3-4}=0.6538	ζ_{3-4}=0.33	ζ_{3-4}=0.164

Table 2: Eigenvalues and Damping

the left half plane stabilizing the system. With increasing lookahead, however, the eigenvalues that were initially unstable become less damped. As with the understeering case, there is an ideal lookahead distance that will yield a stable system with appropriate damping characteristics.

Figure 12 shows the system states for an understeering vehicle with varying amounts of lookahead. The virtual force application point and speed are the same as those used in the eigenvalue figures and the initial condition is a lateral offset of $0.5m$ from the lane center. With a lookahead of $10m$ the system is underdamped with a slow natural frequency. When the preview distance is increased to $30m$ the responses look much better. The damping has increased and all states converge to nominal values in a shorter time. Increasing the preview distance to $50m$, however, creates a poorer system response with high frequency oscillations in the states. Table 2 shows the eigenvalues and damping for these three cases of lookahead.

Given a certain application point for the virtual force, a lookahead distance can be chosen that will create a stable, adequately damped system without any artificial controller damping (i.e. damping on $\dot{e}$ and $\dot{\psi}$). The final way to alter the performance of the system is to include controller damping. Adding damping to the velocity states allows the designer to implement full state feedback on the system, giving the freedom to theoretically place the poles at an arbitrary location (of course, there are limits due to actuator capability, bandwidth, etc.).

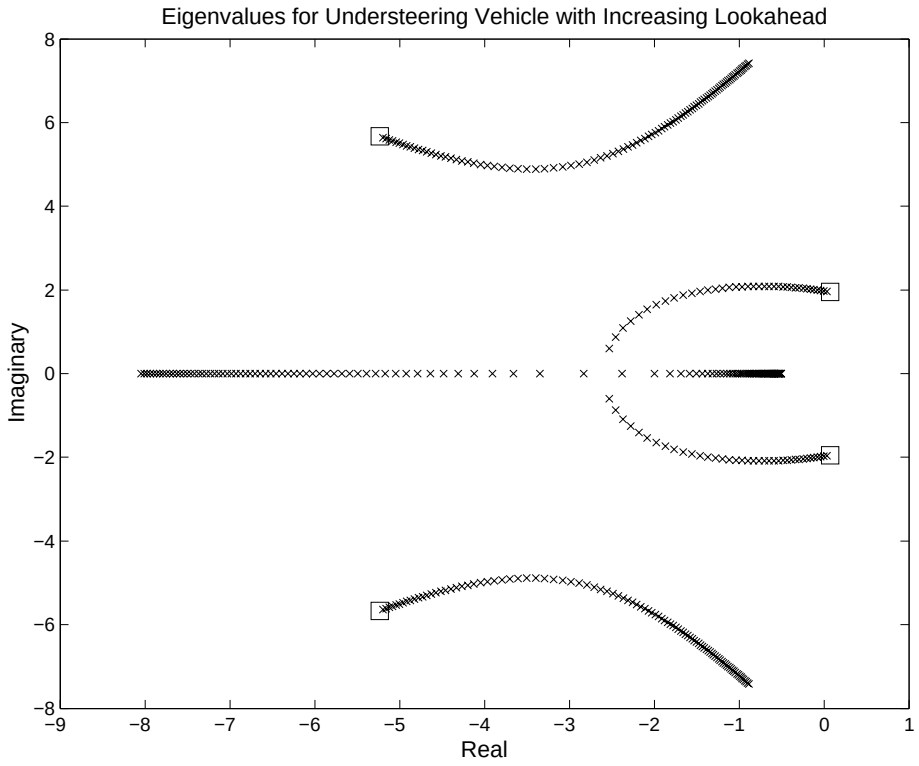

Figure 10: Eigenvalues as the Lookahead Distance is Varied from 0-60m: Understeering Vehicle

7 Controller Damping

If controller damping is added to the system the virtual force is now a function of the lateral position at some lookahead distance, x_{la}, the lateral velocity, $\dot{e}$, and the yaw rate, $\dot{\psi}$.

$$F_{virtual} = -k(e + x_{la}sin\psi) - D_{\dot{e}}\dot{e} - D_{\dot{\psi}}\dot{\psi} \tag{36}$$

where $D_{\dot{e}}$ and $D_{\dot{\psi}}$ are the damping coefficients on the lateral and yaw velocities respectively.

This control law is essentially a proportional derivative controller giving the following linear system.

$$A = \begin{bmatrix} 0 & 1 & 0 & 0 \\ -\frac{k}{m} & \frac{-(C_f+C_r)}{mS} - \frac{\mathbf{D_{\dot{e}}}}{\mathbf{m}} & \frac{C_f+C_r}{m} - \frac{kx_{la}}{m} & \frac{(-aC_f+bC_r)}{mS} - \frac{\mathbf{D_{\dot{\psi}}}}{\mathbf{m}} \\ 0 & 0 & 0 & 1 \\ \frac{-kx_{cf}}{I_z} & \frac{(-aC_f+bC_r)}{I_zS} - \frac{\mathbf{x_{cf}D_{\dot{e}}}}{\mathbf{I_z}} & \frac{(aC_f-bC_r)}{I_z} - \frac{kx_{la}x_{cf}}{I_z} & \frac{-(a^2C_f+b^2C_r)}{I_zS} - \frac{\mathbf{x_{cf}D_{\dot{\psi}}}}{\mathbf{I_z}} \end{bmatrix} \tag{37}$$

If the input is the virtual force from Equation 36 applied at a distance, x_{cf}, from the c.g., the closed loop system can be written as

$$\delta\dot{x} = (A_{OL} - BG)\delta x \tag{38}$$

where A_{OL} is the open loop vehicle dynamics given in Equation 22 with B and G defined as

$$B = \begin{bmatrix} 0 & \frac{1}{m} & 0 & \frac{x_{cf}}{I_z} \end{bmatrix}^T \tag{39}$$

$$G = \begin{bmatrix} k & D_{\dot{e}} & kx_{la} & D_{\dot{\psi}} \end{bmatrix} \tag{40}$$

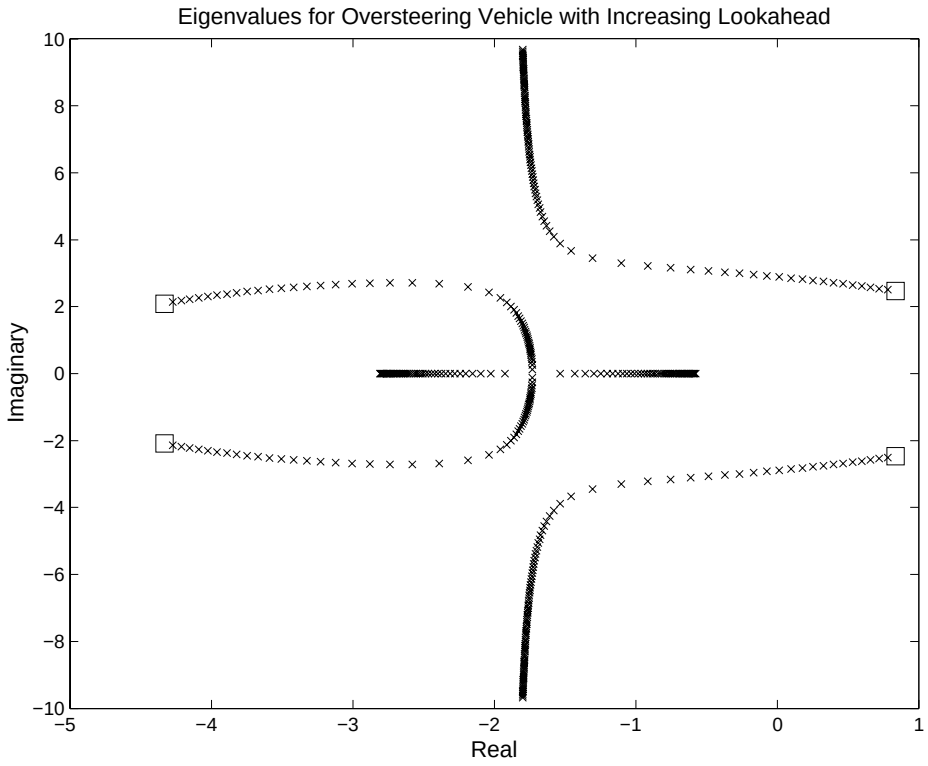

Figure 11: Eigenvalues as the Lookahead Distance is Varied from 0-60m: Oversteering Vehicle

In theory, there is now complete control over the closed loop system dynamics. The poles of the system can be put at any location given the correct choice of the parameters in the virtual force expression. Of course, there are practical limits on these parameters depending on the actuation and sensing capabalities of a particular system. Ignoring these issues, the problem of lateral vehicle control now seems trivial. The gain, lookahead distance, and damping values can be chosen to give any desired response.

In reality, however, it might be undesirable to have large damping values in the controller. With large damping values, the system is constantly losing energy when there is a lateral or yaw velocity. From an efficiency standpoint this is a poor design move. For lanekeeping driver assistance systems, the ability to produce adequate responses without adding any artificial controller damping on the velocity states is quite beneficial. In this case, the control force has a natural association with a positional state corresponding to the edge of the road where control forces are desired to assist the driver.

In cases where damping is undesirable or where lookahead is unavailable full state feedback is not possible. Therefore, the controller will not be able to use certain inputs to alter the output. In these cases, the entire control space is not available and the results and intuition from the previous sections can be used to design a suitable lateral controller.

8 Concluding Remarks

In the case of vehicle control, it is crucial to pay attention to the application point of virtual control forces. Changes in vehicle properties can have deleterious effects on the systems performance and stability. The analysis in this paper illustrates the instabilities that can occur when virtual control forces are applied to a vehicle. This paper looked at three main contributions to lateral stability

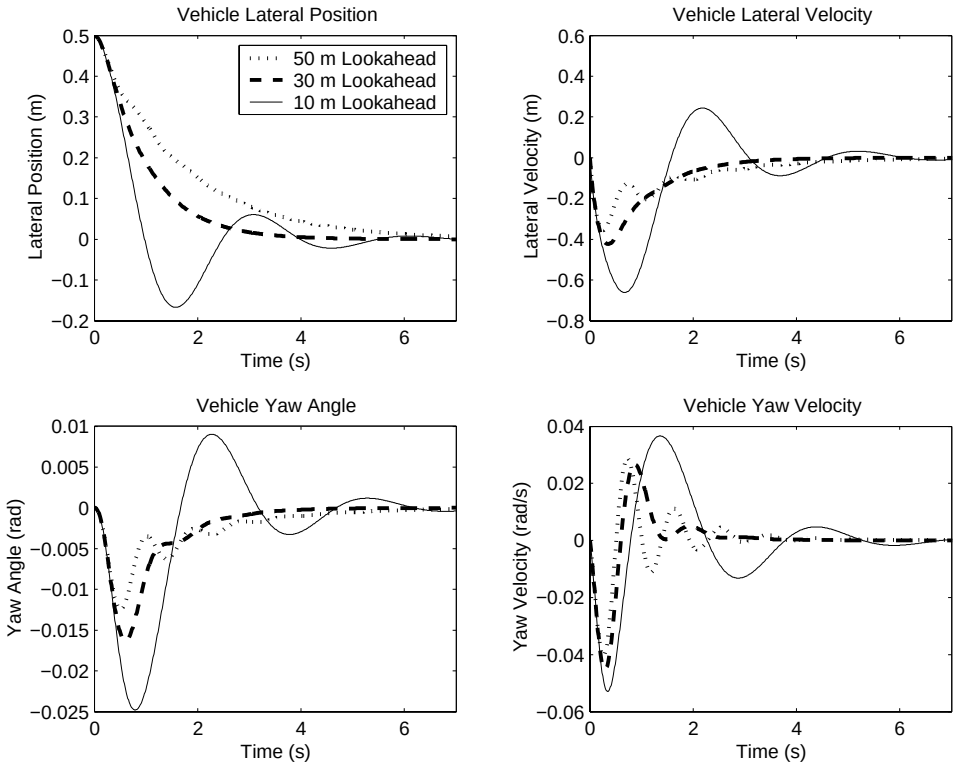

Figure 12: Understeering Vehicle Response with Varying Lookahead

and performance.

- The virtual control force must be applied in front of the neutral steer point
- Lookahead provides adequate performance without controller damping
- Damping on the velocity states and lookahead offer complete control of the system response

A key advantage of having control over the application point of the force is the ability to use less lookahead. As the appliction point approaches the neutral steer point, lateral sensors on the front of the vehicle could be used to achieve an acceptable response eliminating the need for projecting off the front of the vehicle. Future work includes implementation and experimental validation of these results and their role in driver acceptance of lanekeeping assist systems.

References

[1] S. Shladover, C. Desoer, J. Hedrick, M. Tomizuka, J. Walrand, W. Zhang, D. McMahon, H. Deng, S. Sheikholeslam, and N. McKeown, "Automatic vehicle control developments in the path program," *IEEE Transaction on Vehicular Technology*, vol. 40, no. 1, pp. 114–130, 1991.

[2] R. Fenton and R. Mayhan, "Automated highway studies at the ohio state university-an overview," *IEEE Transaction on Vehicular Technology*, vol. 40, no. 1, pp. 100–113, 1991.

[3] K. Stonex, "Car control factors and their measurement," *SAE Transactions*, vol. 36, pp. 81–93, 1941.

[4] L. Segel, "Research in the fundamentals of automobile control and stability," in *Proceedings of the SAE National Summer Meeting*, 1956, pp. 527–540.

[5] William Milliken and Douglas Milliken, *Race Car Vehicle Dynamics*, SAE International, 400 Commonwealth Dr. Warrendale, PA 15096-0001, 1995.

[6] Thomas D. Gillespie, *Fundamentals of Vehicle Dynamics*, Society of Automotive Engineers, Warrendale, PA, 1992.

[7] R. Fenton, G. Melocik, and K. Olson, "On the steering of automated vehicles: Theory and experiment," *IEEE Transactions on Automatic Control*, vol. 21, no. 3, pp. 306–315, 1976.

[8] W. Zhang and R.E. Parsons, "An intelligent roadway reference system for vehicle lateral guidance/control," in *Proceedings of the American Control Conference*, 1990, pp. 281–286.

[9] J. Guldner, H. Tan, and S. Patwardhan, "Analysis of automatic steering control for highway vehicles with look-down lateral reference systems," *Vehicle System Dynamics*, pp. 243–269, 1996.

[10] H. Peng and M. Tomizuka, "Preview control for vehicle lateral guidance in highway automation," ASME *Journal of Dynamic Systems, Measurement, and Control*, vol. 115, pp. 679–686, December 1993.

[11] A. Alleyne and M. DePoorter, "Lateral displacement sensor placement and forward velocity effects on stabiliity of lateral control of vehicles," in *Proceedings of the American Control Conference*, 1997, pp. 1593–1597.

[12] J. Guldner, W. Sienel, H. Tan, J. Ackermann, S. Patwardhan, and T. Buente, "Robust automatic steering control for look-down reference systems with front and rear sensors," *IEEE Transactions on Control Systems Technology*, vol. 7, no. 1, pp. 2–11, 1999.

[13] J. Ackermann, "Robust decoupling of car steering dynamics with arbitrary mass distribution," in *Proceedings of the American Control Conference*, 1994, pp. 1964–1968.

[14] A. Alleyne, "A comparison of alternative intervention strategies for unintended roadway departure (URD) control," in *Proceedings of AVEC 96, Aachen University of Technology, June, 1996*, 1996, pp. 485–506.

[15] B. Koepele and J. Starkey, "Closed-loop vehicle and driver models for high-speed trajectory following," in *Transportation Systems - 1990 ASME WAM, Dallas, TX*, 1990, pp. 59–68.

[16] J.C. Gerdes and E.J. Rossetter, "A unified approach to driver assistance systems based on artificial potential fields," in *Proceedings of the 1999 ASME IMECE, Nashville, TN.*, 1999.

[17] M. Hennessey, C. Shankwitz, and M. Donath, "Sensor based 'virtual bumpers' for collision avoidance: Configuration issues," in *Proceedings of the SPIE*, 1995, vol. 2592.

[18] B. Schiller, V. Morellas, and M. Donath, "Collision avoidance for highway vehicles using the virtual bumper controller," in *Proceedings of the IEEE International Symposium on Intelligent Vehicles*, 1998.

[19] B. Schiller, Y. Du, C. Shankwitz, and M. Donath, "Vehicle guidance architecture for combined lane tracking and obstacle avoidance," in *Artificial Intelligence and Mobile Robots: Case Studies of Successful Robot Systems*, 1998, pp. 159–192.

[20] D. Swaroop and S. Yoon, "Integrated lateral and longitudinal vehicle control for an emergency lane change manoeuvre design," *International Journal of Vehicle Design*, vol. 21, no. 2, pp. 161–174, 1999.